MCB Accepts, published online ahead of print on 25 November 2013
Mol. Cell. Biol. doi:10.1128/MCB.00910-13

Mapping the protein interaction network for the TFIIB-related factor Brf1 in the RNA polymerase III pre-initiation complex

Seok-Kooi Khoo[1,2], Chih-Chien Wu[2], Yu-Chun Lin[2], Jin-Cheng Lee[2], and Hung-Ta Chen[1,2#]

[1.] Taiwan International Graduate Program, Graduate Institute of Life Sciences, National Defense Medical Center, Taipei, Taiwan, R.O.C.

[2.] Institute of Molecular Biology, Academia Sinica, Taipei, Taiwan, R.O.C.

Correspondence to HT Chen, Institute of Molecular Biology, Academia Sinica, 128 Sec. 2 Academia Rd., Taipei 115, Taiwan, R.O.C.

Phone: + 886 2 27824778, Fax: + 886 2 27826085

E-mail: htchen012@gate.sinica.edu.tw

Running Title: Brf1 protein network in the pre-initiation complex

Keywords: Brf1/ RNA Polymerase III/ transcription initiation/ Bdp1/ C34

Abstract

The TFIIB-related factor Brf1 is essential for RNA polymerase (Pol) III recruitment and open promoter formation in transcription initiation. We site-specifically incorporated non-natural amino acid cross-linker to Brf1 to map its protein interaction targets in the pre-initiation complex (PIC). Our cross-linking analysis in the N-terminal domain of Brf1 indicated a pattern of multiple protein interactions reminiscent of TFIIB in the polymerase active site cleft. In addition to the TFIIB-like protein interactions, the Brf1 cyclin repeats subdomain is in contact with the Pol III-specific C34 subunit. With site-directed hydroxyl radical probing, we further revealed the binding between Brf1 cyclin repeats and the highly conserved region connecting C34 winged-helix domains 2 and 3. In contrast to the N-terminal domain of Brf1, the C-terminal domain contains extensive binding sites for TBP and Bdp1 to hold together the TFIIIB complex on the promoter. Overall, the domain architecture of the PIC derived from our cross-linking data explains how individual structural subdomains of Brf1 integrate the protein network from the Pol III active center to the promoter for transcription initiation.

Introduction

Eukaryotic RNA polymerase (Pol) III transcribes precursor tRNAs, 5S ribosomal RNA, small nuclear RNAs such as U6 and 7SK RNAs, and a number of small nucleolar and microRNAs (1). In yeast (*Saccharomyces cerevisiae*), the Pol III transcription apparatus consists of the 17-subunit Pol III and three other transcription factors: the single-polypeptide TFIIIA, the three-subunit TFIIIB and the six-subunit TFIIIC (2, 3). TFIIIA and TFIIIC function as the promoter recognition factors, and TFIIIB is recruited to the promoter through TFIIIC. TFIIIB is composed of the TFIIB-related factor Brf1, the TATA-box binding protein TBP, and the SANT domain-containing subunit Bdp1. Previous biochemical studies indicated that Brf1 and TBP cooperatively assemble onto DNA upstream of the transcription start site, and Bdp1 binds to the Brf1-TBP-DNA complex mainly through its SANT domain (4-10). The TFIIIB-DNA assembly is required for subsequent Pol III recruitment and transcript initiation. Both Brf1 and Bdp1 have been found to interact with Pol III and function in promoter opening (4, 11-14).

The N-terminal domain of yeast Brf1 (Brf1n; aa. 1-286) contains a zinc ribbon fold (aa. 3-34) and a cyclin-fold repeat subdomain (aa. 83-282) (Figure 1A), both of which are homologous to those in the general transcription factor TFIIB of the Pol II system. Based on biochemical and structural analyses, TFIIB ribbon and cyclin-fold repeats are respectively positioned in the RNA exit tunnel and on the wall domain of Pol II (15-20). In addition, the connecting region between the TFIIB ribbon and cyclin repeat domain is structurally resolved to contain B-reader and B-linker motifs interacting with the polymerase active center.

Based on sequence comparison, the connecting region in Brf1n, which we refer to as N-linker, contains low sequence homology with TFIIB. However, this region might also contribute to the binding of the polymerase active center as previous genetic analyses revealed the involvement of ribbon and N-linker in open complex formation (11, 13).

The C-terminal half of Brf1 (Brf1c) is Pol III-specific and is not conserved among the TFIIB family, which, in addition to Brf1 and TFIIB, also includes Rrn7 (TAF1B in human) in the Pol I system (21-24). Yeast Brf1c (aa. 287-596) contains three homologous sequence blocks, I (aa. 287-304), II (aa. 461-515) and III (aa. 570-596) (Figure 1A), that are conserved in *S. cerevisiae*, *Schizosaccharomyces pombe, Candida albicans, Kluyveromyces lactis* and *Homo sapiens* (22, 25). Brf1c exists mostly as a scaffold that holds together the three TFIIIB subunits (12, 26). In particular, structural analysis of the Brf1-TBP-DNA complex indicated that homology block II is positioned along the convex and lateral surfaces of TBP, and the block also interacts with Bdp1 (5, 6, 10, 22, 26-28). The homology blocks are separated by two non-conserved connecting regions that we refer to as C-linkers 1 and 2 (Figure 1A).

Previous genetic and pairwise protein-protein interaction analyses have identified Brf1 interacting partners. In addition to TBP and Bdp1 of the TFIIIB complex, Brf1 interacts with the τ131 (Tfc4) subunit of TFIIIC and two of the Pol III subunits, C34 and C17 (29-33). However, most of the previous studies involved large protein fragments of Brf1, and a detailed and more precise characterization of the Brf1 protein network is not yet available. In this study, we

84 site-specifically incorporated a non-natural photo-reactive amino acid *p*-benzoyl-
85 *L*-phenylalanine (BPA) to the yeast Brf1 to map protein-protein interactions within
86 the Pol III pre-initiation complex (PIC). BPA incorporated in the amino acid
87 sequence of Brf1n revealed cross-linking with TBP and the C160 and C128
88 subunits of the Pol III active site cleft as well as two smaller subunits, C34 and
89 C17. The Brf1-C34 interaction was further analyzed by site-specific hydroxyl
90 radical analysis that revealed the connection between the Brf1 cyclin repeat
91 subdomain and a conserved sequence C-terminal to C34 winged-helix domain 2.
92 Our cross-linking results for Brf1c identified additional Bdp1 and TBP interactions
93 in the C-linker 1 region. Mutational analysis indicated that a Bdp1-binding block
94 in C-linker 1 is required for optimal cell growth and in vitro transcription activity.
95 Overall, our work provides a precise mapping of the network of protein-protein
96 interactions for Brf1 and further elucidates the domain architecture of the Pol III
97 PIC.

Materials and Methods

Yeast strains and plasmids

Yeast strains used for this study were derived from BY4705 with chromosomal disruptions of individual genes by the KanMX4 cassette, yielding Brf1 shuffle strain YSK1 [*MATα ade2::his3G his3Δ200 leu2Δ met15Δ lys2Δ trp1Δ63 ura3Δ* (*brf1*::*KanMX4*) *Brf1*-pRS316 (*URA3*$^+$)] and C34 shuffle strain YLy3 [*MATα ade2::his3G his3Δ200 leu2Δ met15Δ lys2Δ trp1Δ63 ura3Δ* (*Rpc34*::*KanMX4*) *Rpc34*-pRS316 (*URA3*$^+$)] (34, 35). *Brf1* and *Rpc34* (C34) were separately cloned into yeast 2 micron vector pRS425 with *LEU2* selection marker (36). Both genes were driven by yeast *ADH1* promoter. *Brf1* was either V5- or 13-Myc-epitope tagged at the C-terminus via the QuikChange II Site-Directed Mutagenesis Kit (Stratagene), yielding plasmids pSK1 (*Adh1-Brf1*cV5-pRS425) and pSK2 (*Adh1-Brf1*c13Myc-pRS425), respectively. C34 was C-terminally V5-tagged, yielding pYL5 (*Rpc34*cV5-pRS425). Each of the constructed plasmids was used to generate individual mutant plasmids containing single "TAG" (amber) nonsense codon substitution at intended amino acid positions. To generate yeast strains for incorporating non-natural amino acids *p*-benzoyl-*L*-phenylalanine (BPA) into Brf1 and C34, we applied plasmid shuffling to transform individual amber plasmids into yeast YSK1 together with the plasmid pLH157 encoding a suppressor $tRNA_{CUA}$ (corresponding to TAG amber codon) and a BPA-tRNA synthetase (16, 37).

For *Brf1* mutagenesis study, the gene encoding *Brf1* along with its endogenous promoter was cloned into the vector pRS315 with a single HA

epitope tag at the C-terminus, yielding pSK3 (*Brf1*-HA, *ars cen, LEU2*) (38). All *Brf1* mutant plasmids were generated based on pSK3, and the plasmids were transformed into the Brf1 shuffle strain to generate mutant strains by the 5-FOA drop-out method. For cells growth assay, both the WT and mutant strains were grown in YPD till OD_{600} 1.0, and the cell cultures were subsequently diluted with the dilution range of 10^{-2}, 10^{-4} and 10^{-6}. The diluted cells were spotted on the synthetic complete glucose plate lacking leucine, and the growth phenotypes at temperatures 16 °C, 25 °C, 30 °C, and 37 °C were monitored. The incubation time for cell growth at 30 °C and 37 °C was 3 days. For subsequent biochemical studies, yeast whole cell extract (WCE) is prepared. Detailed procedures for preparation of WCE from individual BPA-incorporated or mutant yeast strains have been described previously (14, 39).

PIC isolation and BPA photo-crosslinking

The Pol III pre-initiation complex (PIC) was isolated using the immobilized template assay (IMT) with yeast WCE and DNA template containing either the U6 snRNA or SUP4 tRNA promoter immobilized on Streptavidin magnetic beads (DynaI) as previously described (14, 39). For the BPA photo-crosslinking experiment, 800 μg of WCE was incubated with 4 μg of DNA template immobilized on 200 μg of DynaI beads (Invitrogen) at 30°C for 30 min. Each reaction was washed three times with transcription buffer containing 20 mM K•Hepes (pH7.9), 80 mM KCl, 5 mM $MgCl_2$, 1 mM EDTA, 2%(vol/vol) glycerol, and 0.01% Tween 20. After washing, the reaction was divided into two fractions,

one that would receive UV irradiation (+UV) and the other that would serve as a control (-UV). UV irradiation was conducted with a total energy of 6500 μJ/cm^2 in a Spectrolinker XL-1500 UV oven (Spectronics). The samples were then resuspended in NuPAGE sample buffer (Invitrogen) for SDS-PAGE and Western analysis. The Western blot was visualized with the LICOR Odyssey infrared imaging system using fluorescent dye-labeled secondary antibodies.

In vitro transcription

In vitro transcription was conducted with the IMT assay as described above. After washing, the isolated PICs were resuspended in 17 μL of transcription buffer containing 200 ng α-amanitin, 4 units of RNase inhibitor (Promega), and 1 mM DTT. A mixture of NTPs (3 μL) was subsequently added, and the resulting reaction mixture contains 500 μM each of ATP, UTP, CTP, 50 μM GTP and 0.16 μM [α-^{32}P] GTP (3000 Ci/mmol). After allowing the reaction to proceed at 30^{o}C for 30 min, transcription was quenched by adding 180 μL of 0.1 M sodium acetate, 10 mM EDTA, 0.5% SDS and 200 μg/mL glycogen. The transcripts were extracted by phenol/chloroform and ethanol precipitated, separated on 6% (wt/vol) denaturing urea polyacrylamide gel and visualized by autoradiogram. Restoration of transcription activity was conducted by adding recombinant Brf1 (160 ng) into the Brf1 mutants WCE.

Immunoprecipitation

Brf1 wild-type (WT) and mutant WCEs containing Bdp1 C-terminal Flag-tag and

Brf1 C-terminal HA-tag were used for immunoprecipitation (IP). WCE (1 mg) was mixed with 50 μL of anti-Flag agarose beads (Sigma) in the extract dialysis buffer containing 20 mM K•HEPES pH 7.9, 100 mM KCl, 5 mM $MgCl_2$, 1 mM EDTA, and 20% glycerol and incubated overnight at 4°C. Following 3 washes with 500 μL of extract dialysis buffer, the bound proteins were eluted by boiling the beads at 95°C for 5 min in 20 μL of 4X NuPAGE buffer (Invitrogen). The eluted proteins were resolved by SDS-PAGE and analyzed by Western blot analysis probing with the following antibodies, anti-Flag (probed for Bdp1), anti-HA (probed for Brf1), anti-TBP, and anti-τ131 (Tfc4; TFIIIC subunit).

C34 purification and FeBABE conjugation

Expression and purification of C34 was as described previously (39). To avoid off-target FeBABE conjugation, three endogenous cysteines were altered to non-cysteine residues as follows: Cys124Ala, Cys244Ala and Cys260Ser. All single-cysteine C34 variants were derived from the non-cysteine C34. FeBABE conjugation was performed as described previously (14).

Hydroxyl radical cleavage with C34-FeBABE conjugate

Hydroxyl radical probing in the Pol III PIC was conducted based on the previously established protocol using a C82 mutant WCE allowing dissociation of the C82/34/31 subcomplex from the polymerase core (39). In a IMT reaction, 400 μg yeast WCE containing C-terminally Flag3-tagged Brf1 and the C82 deletion-mutant Δ(50-52) was incubated with 0.72 μg of recombinant C31, 2 μg of

recombinant C82, and 0.94 μg of C34-FeBABE conjugate in a 200 μL reaction containing 2 μg of SUP4 tRNA promoter DNA template. The PICs on beads were washed three times with transcription buffer. After washing, samples were resuspended in 7.5 μL of transcription buffer. The following reagents were added sequentially: 2.5 μL of 50% (vol/vol) glycerol, 1.25 μL of 50 mM sodium ascorbate, and 1.25 μL of H_2O_2 mix [0.24% (vol/vol) H_2O_2, 10mM EDTA]. The hydroxyl radical cleavage reaction was conducted at 30^{o}C for 8 min and quenched by adding 4.5 μL NuPAGE LDS sample buffer (Invitrogen) and 1 μL of 1M DTT. The protein cleavage sites in Brf1 were determined based on the method described previously (14). In vitro transcription analysis was also conducted in parallel. The C34-FeBABE conjugates restored transcription activity similar to that of the wild-type (data not shown).

Results

Brf1 N-terminal domain interacts with Pol III in a similar mode as the TFIIB-Pol II complex

To map the protein-protein interaction network of Brf1, we applied the nonsense suppression method to incorporate BPA site-specifically to the entire Brf1 (37, 40). We generated individual yeast strains each containing a single TAG amber codon in the Brf1 coding sequence for BPA replacement at the designated amino acid positions. A total of 197 strains were created as listed in Table S1. We isolated yeast WCEs from these Brf1-BPA strains and conducted the immobilized template (IMT) assay coupled with UV-irradiation to allow site-specific photo-cross-linking in the isolated PICs. The cross-linking samples were subsequently applied to SDS-PAGE and Western blotting analyses, and protein cross-links were determined based on the appearance of additional low-mobility gel bands generated by UV-irradiation. As demonstrated in the Western analysis (Figure 1B), BPA substitution in residues Gly44 and Gln62 in the N-linker region of Brf1 generated protein cross-links of the size of ~240 kDa (Fig. 1B; lanes 4 and 6). By subtracting the apparent molecular weight of Brf1, the polypeptide cross-linked to Brf1 was estimated to have molecular weight in the range of 160 to 180 kDa. We confirmed this crosslinked polypeptide to be the largest subunit C160 of Pol III by repeating the photo-cross-linking experiment using WCEs containing C-terminally HA-tagged C160 and probing with anti-HA antibody (Fig. 1B; lanes 10 and 12). Cross-linking to the second largest subunit C128 of Pol III was also observed for BPA substitution in residues Arg85 and Arg149 of the first cyclin fold and residue

Asn18 of the ribbon fold (Fig. 1C and data not shown).

As summarized in Figure 1A, Brf1-C160 and -C128 cross-links are distributed respectively in the N-linker and ribbon/cyclin repeat subdomains. The cross-linking pattern suggests a TFIIB-like binding mode as in the Pol II-TFIIB structural model (20). In the Pol II-TFIIB model, the linker region of TFIIB, including B-reader and B-linker motifs, are positioned in the polymerase active center contacting the lid, rudder, and clamp coiled-coil motifs of Rpb1 (homologous to C160). In addition, the first cyclin fold of TFIIB is in close contact with the wall and protrusion domains of Rpb2 (homologous to C128), and the ribbon fold of TFIIB contacts both Rpb1 and Rpb2 in the RNA exit tunnel (16, 20). To further investigate this TFIIB-like binding mode, we conducted another BPA cross-linking analysis in the wall domain of C128. As demonstrated in Figure 1D, a BPA substitution at His801 of the wall domain generated a cross-link with Brf1, supporting the localization of Brf1 on C128. Although further structural and biochemical analyses are required to determine the structural region of Brf1 in contact with the wall domain of C128, our combined photo-cross-linking results with BPA substituted C128 and Brf1 suggest that the Brf1 N-terminal domain likely has a TFIIB-Pol II binding mode in the PIC.

In addition to cross-linking with the two largest subunits of Pol III, we also observed Brf1-C17 cross-linking for residues Lys5 and His8 in the zinc-binding knuckle of the ribbon domain (Fig. 1A; data not shown). Since C17 dimerizes with C25 to form the stalk subcomplex that localizes adjacent to the RNA exit tunnel (41), the Brf1-C17 cross-link suggests a potential functional link between

Brf1 and the stalk in transcription initiation. Furthermore, we observed a Brf1-TBP cross-link at Lys211 at the H2' helix of the second cyclin fold (Fig. 1A & 1E). This cross-link supports the structural model for the binding of cyclin fold repeats with the TBP-DNA complex, where the loop between H2' and H3' helices of the second cyclin fold interacts with the C-terminal stirrup and the C-terminus of TBP (42).

Brf1 cyclin fold repeat subdomain connects with C34 for Pol III recruitment

Our BPA cross-linking analysis for Brf1n revealed subdomain-specific interactions with C160, C128, and TBP, suggesting that Brf1n organizes TFIIB-like domain architecture in the PIC. Based on previous studies with yeast two-hybrid and pull-down analyses, Brf1 also contains a Pol III-system specific interaction with the C34 subunit of the Pol III complex. However, the interaction site for C34 was not precisely mapped as the studies were involved either with the full-length Brf1 protein or with the cyclin fold repeats (aa. 90-262) (22, 43). Consistent with the low-resolution protein mapping data, we observed a weak cross-link between Brf1 and the C34 subunit of Pol III at residue Tyr99 of the H2 helix in the first cyclin fold (Figure 2A).

Our previous cross-linking analysis on Pol III identified inter-subunit interactions that localize C34 N-terminal winged-helix domains WH1 and WH2 above the Pol III active center cleft and the C-terminal region beneath the polymerase clamp domain (Figure 2B). However, it remains unclear how C34 provides additional Pol III-Brf1 interaction for Pol III recruitment as indicated in

previous studies (22, 29, 44). To address this, we incorporated BPA in C34 to map Brf1 binding sites. BPA substitution at Glu169, located at the connecting region between WH2 and the predicted WH3, resulted in a weak cross-link with Brf1 (Figure 2C). Surprisingly, Glu169 is located near the amino acid stretch Asp171-Glu173 that is functionally important for Pol III recruitment (44).

To further characterize the C34-Brf1 interaction, we applied site-directed hydroxyl radical analysis to probe the structural region of Brf1 near the C34 WH2/3 connecting region. We generated C34 single cysteine mutants to conjugate the hydroxyl radical reagent FeBABE at the amino acid positions Leu170 and Ile172. The FeBABE-conjugated C34 variants were applied to the IMT assay for hydroxyl radical protein cleavage analysis in the PIC. In Figure 2D, a Brf1 cleavage fragment was commonly generated by the C34-FeBABE conjugates (Figure 2D; lanes 2, 3, and 4). By comparing with the molecular weight ladder generated from in vitro translated Brf1 peptide fragments, the cleavage site was determined to be in the H4' helix of Brf1n second cyclin fold. In summary, the combined cross-linking and hydroxyl radical analyses suggest an interaction between the WH2/3 connecting region of C34 and the cyclin fold repeats of Brf1n. As the biochemical probing results were weak, we suspect that C34 might not strongly interact with Brf1 in the PIC. However, as previous studies suggested that BPA is a less efficient cross-linking reagent due to its geometry requirement for hydrogen abstraction by benzophenone (45), the weak C34-Brf1 crosslinking could also be attributed to the poor cross-linking efficiency of BPA.

Brf1 C-terminal domain contains extended Bdp1 and TBP binding region

The homology block II of Brf1c serves as the dominant binding site for both TBP and Bdp1, and this block adopts a “vine-on-a-tree” conformation to interact with TBP from the convex surface to the lateral surface of the first structural repeat (6, 27, 28). Consistent with the protein interaction model, our BPA cross-linking analysis conducted in homology block II revealed cross-links with Bdp1 and TBP. As indicated in the summary of Brf1c cross-linking (Figure 3A) and illustrated in Figure 3B, BPA-substitution at residue His473 generates two cross-links confirmed to be TBP and Bdp1, indicating simultaneous interactions with both proteins. Similar simultaneous cross-linking was also observed for BPA substitution at the neighboring residue Ala472 (data not shown). In the homology block II-TBP-DNA ternary complex structure, His473 and Ala472 belong to the helix H23 that interacts with the convex surface of the TBP first structural repeat. Our cross-linking results therefore further suggest the localization for Bdp1 on the TBP convex surface.

Additional Bdp1 and TBP cross-links were also observed for BPA substitutions in the connecting region between homology blocks I and II, which we refer to as C-linker 1. As shown in Figure 3C and summarized in Figure 3A, BPA incorporated at residues Lys319 and Lys335 generated Bdp1 cross-linking. In contrast to the Brf1-Bdp1 cross-links that are clustered closer to homology block I, Brf1-TBP cross-linking occurs at residues widely distributed in C-linker 1 (Figure 3D and summarized in Figure 3A).

The Bdp1-binding block is important for transcription initiation

On the basis of extensive TBP and Bdp1c interactions revealed by BPA cross-linking, we introduced a series of truncations and point mutations in Brf1c. Internal truncations and point mutations were initially introduced in homology block I resulting in cell lethality. In contrast, most of the mutations in C-linker 1 resulted in yeast strains without observable temperature-dependent growth defects. However, mutations in the sequence block Gln311-Arg350, which provided multiple cross-linking with Bdp1 (Figure 3A), conferred a temperature-sensitive growth phenotype. As demonstrated in Figure 4A, the yeast strains with either Leu332Glu point mutation or *del* (Glu331-Tyr340) internal truncation showed slow cell growth at the non-permissive temperature 37°C. We isolated WCEs from these two mutant strains and conducted a co-immunoprecipitation assay to analyze Brf1-Bdp1 binding. As shown in Figure 4B and 4C, both Brf1c mutants severely compromised the binding with Bdp1, supporting our cross-link data. We further analyzed this newly identified Bdp1-binding block by in vitro transcription and PIC formation assays on the SUP4 DNA template. Both mutations severely compromised transcription activity (Figure 4D, lanes 2 and 3). The mutations also caused reduced Bdp1 and Brf1 protein levels in the isolated PICs from the IMT assay (Figure 4E, lanes 2 and 3), indicating that both mutations affect stable association of Bdp1 and Brf1 in the PIC. Our results thus suggest that this Bdp1-binding block provides important structural support for stabilizing Brf1 and Bdp1 in the PIC.

Discussion

In the Pol III transcription machinery, Brf1 together with TBP and Bdp1 constitutes transcription factor TFIIIB for Pol III recruitment and open promoter complex formation. Using site-specific biochemical probing analyses in this study, we precisely mapped the network of protein interactions for Brf1 in the PIC. Our cross-linking results suggest that the Brf1 N-terminal domain organizes a TFIIB-like domain architecture in the PIC. In contrast, the C-terminal half of Brf1 serves mainly as the interface to hold TBP and Bdp1 for TFIIIB complex. An open promoter model for the Pol III PIC is thus derived based on the x-ray structures of Pol II-TFIIB, TFIIB cyclin folds-TBP-DNA, and Brf1 homology block II-TBP-DNA complexes (Figure 5) (20, 28, 46). In the model, the ribbon and the cyclin fold repeat subdomains are respectively localized in the RNA exit tunnel and on the wall domain of polymerase. TBP contacts a 8-bp-long DNA sequence that starts from 30 bases upstream of the transcription start site, and the Brf1 cyclin folds clamp the second stirrup of TBP and interact with DNA sequences flanking the TBP-binding region. Brf1 N-linker region was not modeled due to the lack of structural information. However, this region likely interacts with the open promoter region as well as structural motifs of the active center based on our Brf1-C160 cross-linking and its functional role, together with the ribbon subdomain, in DNA opening (11, 13, 47, 48).

The domain architecture of Pol III derived from our previous study localizes the TFIIE-like C82 and C34 subunits on the polymerase clamp (Figure 5). The WH2 domain of C34 is in close contact with the clamp coiled-coil and

363 further interacts with the upstream edge of the transcription bubble, which is a
364 10~12 base strand-separated promoter region spanning upstream beginning
365 from the transcription start site (39). With the localization of C34 WH2 domain,
366 the functionally important connecting region immediately C-terminal to WH2 is
367 likely positioned adjacent to the Brf1 cyclin fold repeat subdomain. Our site-
368 specific cross-linking and hydroxyl radical data support this interaction. Further,
369 this C34 connecting region likely contributes to additional upstream C34-DNA
370 interaction based on the Pol III-DNA topography analysis indicating co-
371 localization of C34 and Brf1 in the promoter region spanning ~20 bases upstream
372 of the transcription start site (49, 50). In the Pol II PIC, the TFIIB cyclin folds were
373 found to interact with Tfg1 and Tfg2 subunits of the transcription factor TFIIF (15),
374 which is positioned on the lobe and protrusion domains of polymerase (40).
375 Compared to TFIIE, which also interacts with the polymerase clamp, the
376 localization of TFIIF is on the opposite side of the polymerase cleft. Therefore,
377 the cyclin repeats domain is involved in establishing specific interactions with
378 polypeptides on the polymerase active center cleft for respective transcription
379 systems.

380 Our cross-linking data indicate Brf1c mainly serves as a bipartite interface
381 for TBP and Bdp1. Specifically, our analysis extends Bdp1- and TBP-binding
382 sites to the C-linker 1 region, and we identified a functionally important Bdp1-
383 binding sequence block. Although this Bdp1-binding block contains low sequence
384 homology, secondary structure analysis indicates consensus α-helical secondary
385 structures in this region. Furthermore, this Bdp1-binding block contains the amino

acid sequence Gly328-Glu329-Gln330-Glu331-Leu332 (GEXEL) that was previously reported to be a conserved short motif in Brf1c (25). The structural region of Bdp1 that interacts with this sequence block remains to be determined. In addition to TBP and Bdp1 interactions, we observed a weak C34 cross-link for BPA substitution at Gln549 adjacent to homology block III (data not shown). This C34 cross-link supports a previous genetic interaction analysis that mapped Brf1-C34 interaction to homology blocks II and III (29).

The domain architecture of the PIC derived from this study explains respective functional roles in DNA opening for ribbon and N-linker and in organizing TFIIIB-pol III-DNA complex for the cyclin fold repeats subdomain and the C-terminal domain. In the eukaryotic Pol I system, the TFIIB-related factors TAF1B in human and Rrn7 in yeast also contain TFIIB-like ribbon and cyclin repeat subdomains in their N-terminal domains and unique C-terminal domains specific for respective polymerases (23, 24). Genetic analysis for TAF1B indicated that the zinc ribbon and the connecting region (N-terminal linker) mainly function in post-recruitment step(s), reminiscent of Brf1 (23). Although the analysis for domain localization is not available, a conserved binding mechanism may exist for these Pol I factors as suggested by our study for Brf1.

Acknowledgements

We thank Dr. George Kassavetis (UC San Diego) for advices on biochemical probing experiments. We thank Yue-Chang Chou for protein purification. We thank AndreAna Peña for English editing. This work was supported by the grant NSC 100-2311-B-001-013-MY3 from National Science Council, R.O.C. and the Career Development Award to H.-T.C. from Academia Sinica.

References

1. **Dieci, G., G. Fiorino, M. Castelnuovo, M. Teichmann, and A. Pagano.** 2007. The expanding RNA polymerase III transcriptome. Trends Genet **23:**614-622.
2. **Geiduschek, E. P., and G. A. Kassavetis.** 2001. The RNA polymerase III transcription apparatus. J Mol Biol **310:**1-26.
3. **Schramm, L., and N. Hernandez.** 2002. Recruitment of RNA polymerase III to its target promoters. Genes Dev **16:**2593-2620.
4. **Ishiguro, A., G. A. Kassavetis, and E. P. Geiduschek.** 2002. Essential roles of Bdp1, a subunit of RNA polymerase III initiation factor TFIIIB, in transcription and tRNA processing. Mol Cell Biol **22:**3264-3275.
5. **Kassavetis, G. A., C. Bardeleben, A. Kumar, E. Ramirez, and E. P. Geiduschek.** 1997. Domains of the Brf component of RNA polymerase III transcription factor IIIB (TFIIIB): functions in assembly of TFIIIB-DNA complexes and recruitment of RNA polymerase to the promoter. Mol Cell Biol **17:**5299-5306.
6. **Kassavetis, G. A., R. Driscoll, and E. P. Geiduschek.** 2006. Mapping the principal interaction site of the Brf1 and Bdp1 subunits of Saccharomyces cerevisiae TFIIIB. J Biol Chem **281:**14321-14329.
7. **Kumar, A., A. Grove, G. A. Kassavetis, and E. P. Geiduschek.** 1998. Transcription factor IIIB: the architecture of its DNA complex, and its roles in initiation of transcription by RNA polymerase III. Cold Spring Harb Symp Quant Biol **63:**121-129.
8. **Kumar, A., G. A. Kassavetis, E. P. Geiduschek, M. Hambalko, and C. J. Brent.** 1997. Functional dissection of the B" component of RNA polymerase III transcription factor IIIB: a scaffolding protein with multiple roles in assembly and initiation of transcription. Mol Cell Biol **17:**1868-1880.
9. **Librizzi, M. D., M. Brenowitz, and I. M. Willis.** 1998. The TATA element and its context affect the cooperative interaction of TATA-binding protein with the TFIIB-related factor, TFIIIB70. The Journal of biological chemistry **273:**4563-4568.
10. **Saida, F.** 2008. Structural characterization of the interaction between TFIIIB components Bdp1 and Brf1. Biochemistry **47:**13197-13206.
11. **Kassavetis, G. A., A. Kumar, G. A. Letts, and E. P. Geiduschek.** 1998. A post-recruitment function for the RNA polymerase III transcription-initiation factor IIIB. Proc Natl Acad Sci U S A **95:**9196-9201.
12. **Kassavetis, G. A., A. Kumar, E. Ramirez, and E. P. Geiduschek.** 1998. Functional and structural organization of Brf, the TFIIB-related component of the RNA polymerase III transcription initiation complex. Mol Cell Biol **18:**5587-5599.
13. **Hahn, S., and S. Roberts.** 2000. The zinc ribbon domains of the general transcription factors TFIIB and Brf: conserved functional surfaces but different roles in transcription initiation. Genes Dev **14:**719-730.
14. **Wu, C. C., Y. C. Lin, and H. T. Chen.** 2011. The TFIIF-like Rpc37/53 dimer lies at the center of a protein network to connect TFIIIC, Bdp1, and the RNA polymerase III active center. Molecular and cellular biology **31:**2715-2728.
15. **Chen, H. T., and S. Hahn.** 2004. Mapping the location of TFIIB within the RNA

polymerase II transcription preinitiation complex: a model for the structure of the PIC. Cell **119:**169-180.

16. **Chen, H. T., and S. Hahn.** 2003. Binding of TFIIB to RNA polymerase II: Mapping the binding site for the TFIIB zinc ribbon domain within the preinitiation complex. Mol Cell **12:**437-447.
17. **Bushnell, D. A., K. D. Westover, R. E. Davis, and R. D. Kornberg.** 2004. Structural basis of transcription: an RNA polymerase II-TFIIB cocrystal at 4.5 Angstroms. Science **303:**983-988.
18. **Liu, X., D. A. Bushnell, D. Wang, G. Calero, and R. D. Kornberg.** 2010. Structure of an RNA polymerase II-TFIIB complex and the transcription initiation mechanism. Science **327:**206-209.
19. **Kostrewa, D., M. E. Zeller, K. J. Armache, M. Seizl, K. Leike, M. Thomm, and P. Cramer.** 2009. RNA polymerase II-TFIIB structure and mechanism of transcription initiation. Nature **462:**323-330.
20. **Sainsbury, S., J. Niesser, and P. Cramer.** 2012. Structure and function of the initially transcribing RNA polymerase II-TFIIB complex. Nature.
21. **Colbert, T., and S. Hahn.** 1992. A yeast TFIIB-related factor involved in RNA polymerase III transcription. Genes Dev **6:**1940-1949.
22. **Khoo, B., B. Brophy, and S. P. Jackson.** 1994. Conserved functional domains of the RNA polymerase III general transcription factor BRF. Genes Dev **8:**2879-2890.
23. **Naidu, S., J. K. Friedrich, J. Russell, and J. C. Zomerdijk.** 2011. TAF1B is a TFIIB-like component of the basal transcription machinery for RNA polymerase I. Science **333:**1640-1642.
24. **Knutson, B. A., and S. Hahn.** 2011. Yeast Rrn7 and human TAF1B are TFIIB-related RNA polymerase I general transcription factors. Science **333:**1637-1640.
25. **Martinez, M. J., and K. U. Sprague.** 2003. Cloning of a putative Bombyx mori TFIIB-related factor (BRF). Arch Insect Biochem Physiol **54:**55-67.
26. **Kassavetis, G. A., C. A. Joazeiro, M. Pisano, E. P. Geiduschek, T. Colbert, S. Hahn, and J. A. Blanco.** 1992. The role of the TATA-binding protein in the assembly and function of the multisubunit yeast RNA polymerase III transcription factor, TFIIIB. Cell **71:**1055-1064.
27. **Colbert, T., S. Lee, G. Schimmack, and S. Hahn.** 1998. Architecture of protein and DNA contacts within the TFIIIB-DNA complex. Mol Cell Biol **18:**1682-1691.
28. **Juo, Z. S., G. A. Kassavetis, J. Wang, E. P. Geiduschek, and P. B. Sigler.** 2003. Crystal structure of a transcription factor IIIB core interface ternary complex. Nature **422:**534-539.
29. **Andrau, J. C., A. Sentenac, and M. Werner.** 1999. Mutagenesis of yeast TFIIIB70 reveals C-terminal residues critical for interaction with TBP and C34. J Mol Biol **288:**511-520.
30. **Ferri, M. L., G. Peyroche, M. Siaut, O. Lefebvre, C. Carles, C. Conesa, and A. Sentenac.** 2000. A novel subunit of yeast RNA polymerase III interacts with the TFIIB-related domain of TFIIIB70. Mol Cell Biol **20:**488-495.
31. **Moir, R. D., K. V. Puglia, and I. M. Willis.** 2000. Interactions between the tetratricopeptide repeat-containing transcription factor TFIIIC131 and its ligand,

TFIIIB70. Evidence for a conformational change in the complex. J Biol Chem **275:**26591-26598.

32. **Moir, R. D., K. V. Puglia, and I. M. Willis.** 2002. Autoinhibition of TFIIIB70 binding by the tetratricopeptide repeat-containing subunit of TFIIIC. J Biol Chem **277:**694-701.
33. **Moir, R. D., I. Sethy-Coraci, K. Puglia, M. D. Librizzi, and I. M. Willis.** 1997. A tetratricopeptide repeat mutation in yeast transcription factor IIIC131 (TFIIIC131) facilitates recruitment of TFIIB-related factor TFIIIB70. Mol Cell Biol **17:**7119-7125.
34. **Brachmann, C. B., A. Davies, G. J. Cost, E. Caputo, J. Li, P. Hieter, and J. D. Boeke.** 1998. Designer deletion strains derived from Saccharomyces cerevisiae S288C: a useful set of strains and plasmids for PCR-mediated gene disruption and other applications. Yeast **14:**115-132.
35. **Wach, A., A. Brachat, R. Pohlmann, and P. Philippsen.** 1994. New heterologous modules for classical or PCR-based gene disruptions in Saccharomyces cerevisiae. Yeast **10:**1793-1808.
36. **Christianson, T. W., R. S. Sikorski, M. Dante, J. H. Shero, and P. Hieter.** 1992. Multifunctional yeast high-copy-number shuttle vectors. Gene **110:**119-122.
37. **Chin, J. W., T. A. Cropp, J. C. Anderson, M. Mukherji, Z. Zhang, and P. G. Schultz.** 2003. An expanded eukaryotic genetic code. Science **301:**964-967.
38. **Sikorski, R. S., and P. Hieter.** 1989. A system of shuttle vectors and yeast host strains designed for efficient manipulation of DNA in Saccharomyces cerevisiae. Genetics **122:**19-27.
39. **Wu, C. C., F. Herzog, S. Jennebach, Y. C. Lin, C. Y. Pai, R. Aebersold, P. Cramer, and H. T. Chen.** 2012. RNA polymerase III subunit architecture and implications for open promoter complex formation. Proc Natl Acad Sci U S A **109:**19232-19237.
40. **Chen, H. T., L. Warfield, and S. Hahn.** 2007. The positions of TFIIF and TFIIE in the RNA polymerase II transcription preinitiation complex. Nat Struct Mol Biol **14:**696-703.
41. **Jasiak, A. J., K. J. Armache, B. Martens, R. P. Jansen, and P. Cramer.** 2006. Structural biology of RNA polymerase III: subcomplex C17/25 X-ray structure and 11 subunit enzyme model. Mol Cell **23:**71-81.
42. **Nikolov, D. B., H. Chen, E. D. Halay, A. A. Usheva, K. Hisatake, D. K. Lee, R. G. Roeder, and S. K. Burley.** 1995. Crystal structure of a TFIIB-TBP-TATA-element ternary complex. Nature **377:**119-128.
43. **Werner, M., N. Chaussivert, I. M. Willis, and A. Sentenac.** 1993. Interaction between a complex of RNA polymerase III subunits and the 70-kDa component of transcription factor IIIB. J Biol Chem **268:**20721-20724.
44. **Brun, I., A. Sentenac, and M. Werner.** 1997. Dual role of the C34 subunit of RNA polymerase III in transcription initiation. EMBO J **16:**5730-5741.
45. **Tate, J. J., J. Persinger, and B. Bartholomew.** 1998. Survey of four different photoreactive moieties for DNA photoaffinity labeling of yeast RNA polymerase III transcription complexes. Nucleic acids research **26:**1421-1426.
46. **Tsai, F. T., and P. B. Sigler.** 2000. Structural basis of preinitiation complex assembly on human pol II promoters. Embo J **19:**25-36.

47. **Kassavetis, G. A., G. A. Letts, and E. P. Geiduschek.** 1999. A minimal RNA polymerase III transcription system. EMBO J **18:**5042-5051.
48. **Kassavetis, G. A., G. A. Letts, and E. P. Geiduschek.** 2001. The RNA polymerase III transcription initiation factor TFIIIB participates in two steps of promoter opening. EMBO J **20:**2823-2834.
49. **Bartholomew, B., D. Durkovich, G. A. Kassavetis, and E. P. Geiduschek.** 1993. Orientation and topography of RNA polymerase III in transcription complexes. Mol Cell Biol **13:**942-952.
50. **Bartholomew, B., G. A. Kassavetis, and E. P. Geiduschek.** 1991. Two components of Saccharomyces cerevisiae transcription factor IIIB (TFIIIB) are stereospecifically located upstream of a tRNA gene and interact with the second-largest subunit of TFIIIC. Molecular and cellular biology **11:**5181-5189.

Figure Legends

Figure 1. Brf1n BPA photo-crosslinking. **(A)** Schematic of Brf1 domain architecture and summary of Brf1n BPA photo-crosslinking. Residue numbers for the boundaries of individual subdomains are marked. NL, N-linker; CL-1&2, C-linker 1&2. BPA-substituted residues are color coded according to respective cross-linked polypeptides indicated below the horizontal connecting lines. Lower panel: models of the ribbon fold (left) and the Brf1c homology block II-TBP-DNA complex (right). The magenta sphere in the ribbon model indicates the zinc ion. TBP is displayed with the molecular surface model in light green. Others are shown as backbone trace with Brf1c homology block II in brown, Brf1n cyclin folds in orange, template DNA (TS) in dark blue, and non-template DNA (NTS) in cyan. BPA-substituted residues with confirmed cross-linking targets are highlighted with spheres. The hydroxyl radical cleavage site (Ala246±5aa) in Brf1n by C34-FeBABE is indicated. **(B)** Western analysis of Brf1-C160 photo-cross-linking. BPA-substituted residues are indicated above the lanes. Brf1-C160 cross-linking was identified using anti-V5 antibodies (Brf1) (lanes 1-6) and confirmed with anti-HA antibodies (C160) (lanes 7-12), respectively. Triangles are placed next to the cross-linking gel bands. All cross-linking bands in subsequent figures are marked by triangles. WCE, yeast whole cells extract; UV + or –, with or without UV irradiation; WT, wild-type Brf1 with no BPA replacement; *, non-specific background band. **(C)** Brf1-C128 photo-crosslinking. Brf1-C128 cross-linking band was visualized with anti-V5 antibody (Brf1) (lanes 1-4) and confirmed with anti-HA antibody (C128) (lanes 5-8). **(D)** C128-Brf1 photo-

crosslinking. C128-Brf1 cross-linking band was visualized with anti-Myc antibody (C128) (lanes 1-4) and confirmed with anti-Flag antibody (Brf1) (lanes 5-8). The BPA position in C128 additionally cross-links to C82. **(E)** Brf1-TBP photo-crosslinking at BPA substituted residue Lys211 in the second cyclin fold of Brf1. The cross-linked Brf1-TBP was probed with anti-V5 antibody (Brf1) (lane 1-4) and confirmed by anti-TBP antibody (lane 5-8).

Figure 2. Brf1n cyclin folds interact with C34. **(A)** Brf1-C34 photo-cross-linking from BPA-substitution at residue Tyr99 of Brf1. The cross-linking was visualized with an antibody against V5 (Brf1) (left panel) and was verified with C34 antiserum (right panel). Cross-linking bands are marked with triangles. The bands marked with asterisks (*) are background bands, which appear to be UV-specific. **(B)** Schematic of C34 domain architecture. As highlighted in the sequence of the connecting region between WH2 and 3 domains, Asp171 and Glu173 mutations affect transcription initiation. **(C)** Western analysis of C34-Brf1 cross-linking. BPA-substitution is at the residue Glu169 of C34. Crosslink was visualized by probing with anti-V5 antibody (C34) (left panel) and the identity of the C34-Brf1 cross-linking band was verified by probing with Brf1 antiserum (right panel). Asterisk (*) marks a non-specific background band. **(D)** Determination of C34-FeBABE hydroxyl radical cleavage site in Brf1. The hydroxyl radical cleavage peptide fragment is revealed in the Western blot analysis with anti-Flag antibody, and the cleavage site is determined to be in the cyclin fold repeat subdomain of Brf1 as indicated. The non-cysteine (nonCys) mutant of C34 does

not contain any cysteine residue for FeBABE conjugation and served as the negative control. Non-specific bands are marked with asterisks.

Figure 3. BPA photo-cross-linking in Brf1c. **(A)** Summary of Brf1c BPA photo-crosslinking. **(B)** Western analysis of cross-linking for BPA-substitution at His473 of Brf1. The cross-linking results were probed with anti-V5 antibody (Brf1) (left panel), anti-Flag antibody (TBP) (middle panel), and anti-Bdp1 antibody (right panel). The cross-linking bands are marked with triangles. A slight upper mobility shift for the Brf1-TBP cross-link in the middle panel was caused by the use of Flag epitope tagging in TBP. **(C)** Western analysis of Brf1-Bdp1 cross-linking at Lys319 and Lys335 in the C-linker 1 (CL-1) region. The Western blot was probed with anti-Myc antibody for Myc-epitope tagged Brf1 and anti-Bdp1 antibody to confirm the Bdp1 polypeptide in the cross-linked fusion (lanes 8 and 10). **(D)** Western analysis of Brf1-TBP cross-linking for BPA-substitution at residues Ser420, Gln424 and Asn418 of Brf1c.

Figure 4. Mutational analysis of Brf1c homology block I and C-linker 1. **(A)** Cell growth phenotype was analyzed by the serial dilution spot assay. Both Leu332Glu and *del* (Glu331-Tyr340) mutants showed slower growth at 37^{o}C. **(B)** Western blot analysis of co-immunoprecipitation for Brf1 Leu332Glu and *del* (Glu331-Tyr340) mutants. Co-IP was conducted with anti-Flag agarose to precipitate Flag-tagged Bdp1 and co-immune precipitated polypeptides were probed with respective antibodies indicated on the left. **(C)** IP-anti-Flag results

626 are quantified and plotted with WT signals set to 1. Errors bars indicate s.e.m.
627 from four independent experiments. **(D)** Transcription activity of Brf1 mutants. As
628 indicated, WCEs from wild-type (WT) or mutant yeast strains were used in the in
629 vitro transcription assay. The autoradiograms show the SUP4 pre-tRNA transcript
630 (upper panel) and SnR6 transcript (lower panel). rBrf1, recombinant wild-type
631 Brf1. **(E)** Immobilized template analysis. Proteins in the isolated Pol III PICs from
632 the IMT assay were probed with antibodies as indicated on the left. The relative
633 protein levels for Brf1 and Bdp1 are listed below each gel band.
634
635 **Figure 5.** Model of the Pol III open promoter complex. **(A)** The structural model
636 contains Pol III, Brf1, TBP, and open promoter DNA based on the Pol II-TFIIB-
637 TBP open promoter complex (19, 20) and the Brf1c homology block II-TBP-DNA
638 structure (28). Subdomains of Brf1 are displayed with the backbone trace model
639 and are color-coded: Brf1n cyclin repeats in orange and Brf1c homology block II
640 in brown. The molecular surface model of TBP is colored pale green. The Pol III
641 core structure is shown as the white molecular surface, and the magenta sphere
642 in the active center denotes the magnesium ion. Pol III-specific subunits are
643 displayed as follows: C34 WH1 and WH2, magenta backbone trace; C82, tan
644 molecular surface; C37/53 subcomplex, light blue molecular surface. DNA is
645 represented by the phosphate backbone trace with the template strand in blue
646 and non-template strand in cyan. Positions of DNA base-pairs -38/-39 and -21 on
647 the non-template strand (relative to the transcription start site as +1) are also
648 indicated. The localization for the WH3 domain of C34 is indicated as the dashed

oval line in black. The atomic coordinate file for the Pol III PIC model is available upon request. **(B)** Same as in (A) with rotation as indicated. The molecular surfaces for Pol III core, C37/53 subcomplex, and C82 are semi-transparent. As highlighted with the spheres in the Brf1 cyclin repeats model, Glu98 and Tyr99 provide Brf1-C34 BPA-cross-linking and Ala246 (±5aa) is the hydroxyl radical cleavage site by the FeBABE-conjugated C34. The dashed circle represents the potential localization for the connecting region between the WH2 and WH3 domains of C34.

Figure 1

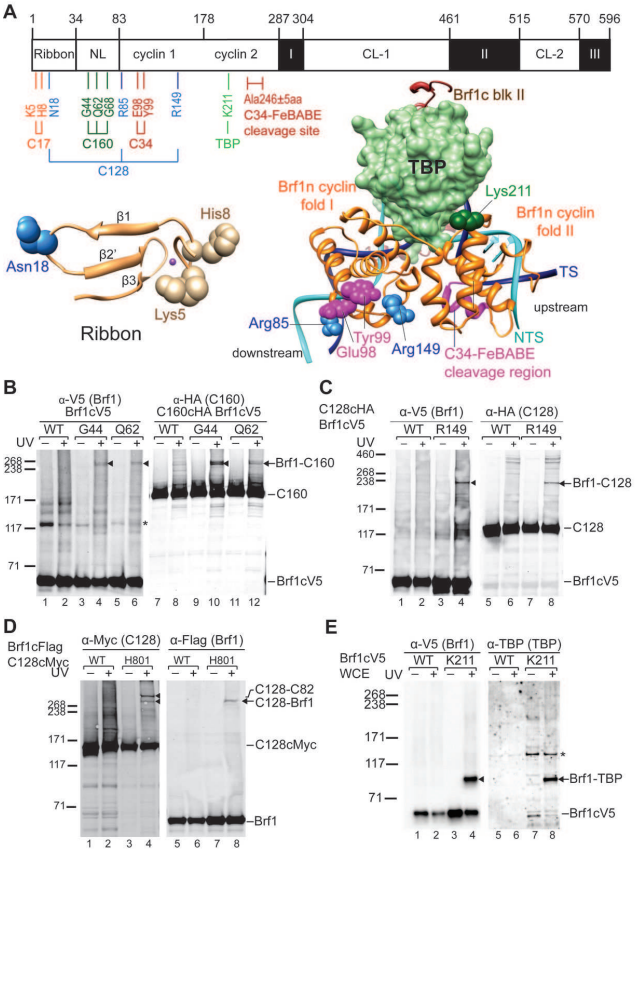

Figure 2

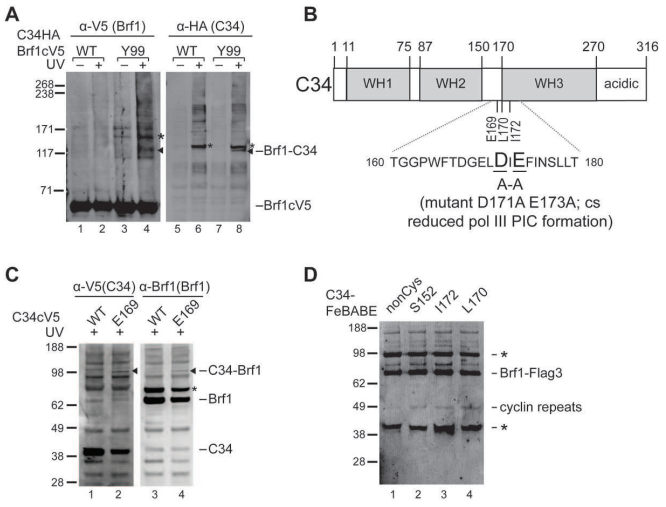

Figure 3

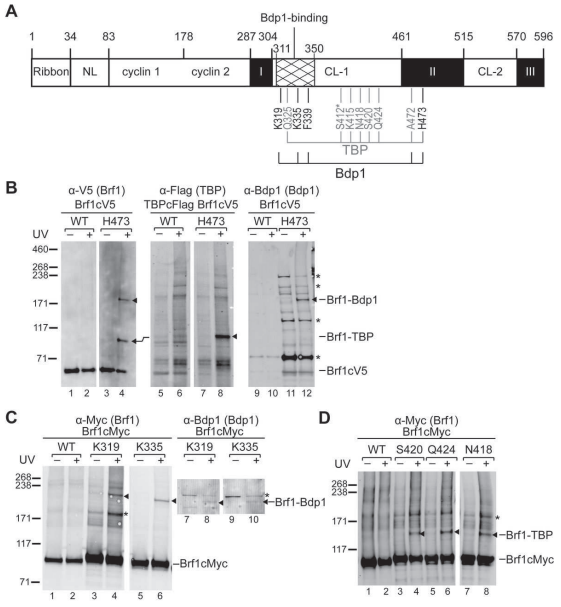

Figure 4

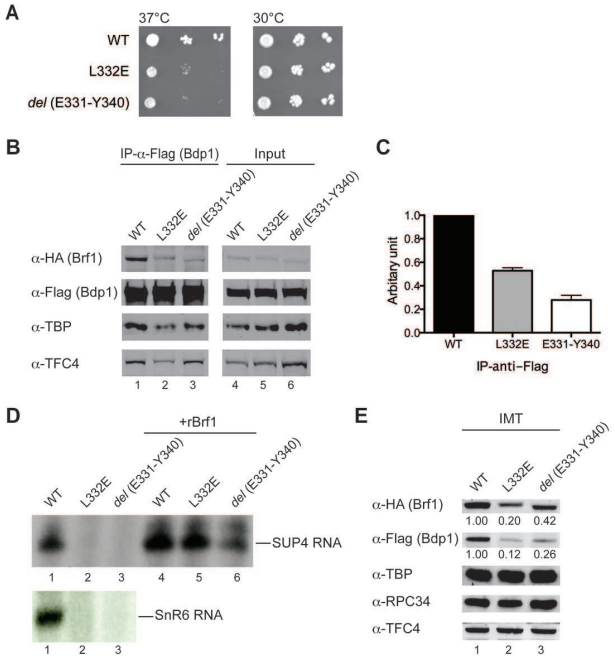

Figure 5